



Analysis of particle size distribution changes

R. Väänänen et al.

This discussion paper is/has been under review for the journal Atmospheric Chemistry and Physics (ACP). Please refer to the corresponding final paper in ACP if available.

Analysis of particle size distribution changes between three measurement sites in Northern Scandinavia

R. Väänänen¹, E.-M. Kyrö¹, T. Nieminen^{1,2}, N. Kivekäs^{3,4}, H. Junninen¹, A. Virkkula^{1,3}, M. Dal Maso^{1,5}, H. Lihavainen³, Y. Viisanen³, B. Svenningsson⁴, T. Holst⁶, A. Arneth⁷, P. P. Aalto¹, M. Kulmala¹, and V.-M. Kerminen¹

¹University of Helsinki, Department of Physics, Helsinki, 00014 University of Helsinki, Finland

²Helsinki Institute of Physics, P.O. Box 64, 00014 University of Helsinki, Finland

³Finnish Meteorological Institute, Climate Change Unit, 00101 Helsinki, Finland

⁴Lund University, Department of Physics, Lund, 22100 Lund, Sweden

⁵Tampere University of Technology, Dept. of Physics, P.O. Box 692, 33101 Tampere, Finland

⁶Department of Physical Geography and Ecosystems Science, Sölvegatan 12, 223 62 Lund, Sweden

⁷Karlsruher Institute of Technology, Institute of Meteorology and Climate Research/Atmospheric Environmental Research (IMK-IFU), Kreuzackbahnstr. 19, 82467 Garmisch-Partenkirchen, Germany

Title Page

Abstract

Introduction

Conclusions

References

Tables

Figures



Back

Close

Full Screen / Esc

Printer-friendly Version

Interactive Discussion



Received: 15 February 2013 – Accepted: 23 March 2013 – Published: 9 April 2013

Correspondence to: R. Väänänen (riikka.vaananen@helsinki.fi)

Published by Copernicus Publications on behalf of the European Geosciences Union.

ACPD

13, 9401–9442, 2013

Analysis of particle size distribution changes

R. Väänänen et al.

Title Page

Abstract

Introduction

Conclusions

References

Tables

Figures



Back

Close

Full Screen / Esc

Printer-friendly Version

Interactive Discussion



Abstract

We investigated atmospheric aerosol particle dynamics in a boreal forest zone in Northern Scandinavia. We used aerosol size distribution data measured with either a Differential Mobility Particle Sizer (DMPS) or Scanning Mobility Particle Sizer (SMPS) at three stations (Värriö, Pallas and Abisko), and combined these data with the HYSPLIT air mass trajectory analysis. We compared three approaches: analysis of new particle formation events, investigation of air masses transport from the ocean to individual stations with different over-land transport times, and analysis of changes in aerosol particle size distributions during the air masses transport from one measurement station to another. Aitken mode particles were found to have an apparent average growth rate of 0.6–0.7 nm h⁻¹ when the air masses travelled over land. Particle growth rates during the NPF events were 3–6 times higher than the apparent particle growth. When comparing aerosol dynamics between the different stations for different over-land transport times, no major differences were found except that in Abisko the new particle formation events were observed to take place in air masses having shorter over-land times than at the other stations. We speculate that this is related to the meteorological differences along the paths of air masses caused by the land surface topology. When comparing between air masses travelling the east-to-west direction to those traveling the west-to-east directions, clear differences in the aerosol dynamics were seen. Our results suggest that the condensation growth has an important role in aerosol dynamics also when new particle formation is not evident.

1 Introduction

High northern latitudes, including the Arctic and large parts of the boreal forest zone, are experiencing much faster surface warming than the Earth as a whole (Lu and Cai, 2010; Screen et al., 2012). Atmospheric aerosol particles play an important, and complex, role in the high-latitude climate system. Firstly, large reductions in anthropogenic

ACPD

13, 9401–9442, 2013

Analysis of particle size distribution changes

R. Väänänen et al.

Title Page

Abstract

Introduction

Conclusions

References

Tables

Figures

◀

▶

◀

▶

Back

Close

Full Screen / Esc

Printer-friendly Version

Interactive Discussion



**Analysis of particle
size distribution
changes**

R. Väänänen et al.

Title Page

Abstract

Introduction

Conclusions

References

Tables

Figures

◀

▶

◀

▶

Back

Close

Full Screen / Esc

Printer-friendly Version

Interactive Discussion



sulfur emissions in Europe and North America have decreased sulfate aerosol concentrations over high latitudes over the past three decades, having thereby enhanced the warming observed over those areas (Shindell and Faluvegi, 2009). Secondly, absorption of solar radiation by black carbon (BC) aerosols is enhanced by highly reflective snow surface (e.g. Law and Stohl 2007) and deposition of black carbon particles onto snow is probably contributing to the positive snow–albedo feedback mechanism that is active over the Arctic during the springtime (Flanner et al., 2009). Thirdly, boreal forests themselves are a major source of biogenic secondary aerosol particles during the summer part of the year (Kulmala et al., 2011; Tunved et al., 2006a). These particles have been estimated to cause a significant cooling effect via their interaction with clouds (Spracklen et al., 2008; Lihavainen et al., 2009), and to be part of a potentially important negative feedback loop in a warming climate (Tunved et al., 2008; Kulmala et al., 2004a).

The cooling potential of secondary particles produced by boreal forests is connected tightly with aerosol dynamical processes taking place during atmospheric transport, especially the particle growth, since secondary particles need to reach diameters larger than about 50–100 nm in order to participate in cloud droplet activation (Kerminen et al., 2005; Komppula et al., 2005; Sihto et al., 2011; Spracklen et al., 2011).

Long-term aerosol measurements conducted at various North European sites have brought plenty of new insight into the formation and growth behavior of boreal forest aerosols (Kulmala et al., 2004b; Vehkamäki et al., 2004; Dal Maso et al., 2007; Svenningsson et al., 2008; Asmi et al., 2011). The problem with these studies is, however, that particle growth rates are obtained only from a subset of days with the most prominent growth, which is very likely to bias the results. Another problem with measurements conducted at fixed sites is that they provide limited amount of information on the mutual interaction between various aerosol dynamical processes during atmospheric transport. Finally, such measurements do not reveal the spatial extent of secondary aerosol formation, or how long it takes to establish a balance between the aerosol formation and removal mechanisms.

Analysis of particle size distribution changes

R. Väänänen et al.

Title Page

Abstract

Introduction

Conclusions

References

Tables

Figures



Back

Close

Full Screen / Esc

Printer-friendly Version

Interactive Discussion

One approach to investigate aerosol dynamics during atmospheric transport is to look for and analyze air mass transport situations between two measurements stations. In the boreal forest environment, this has been done earlier in only a couple of investigations. Komppula et al. (2006) concentrated on new particle formation days in Finnish Lapland. They combined particle size distribution measurements and simulations of aerosol dynamics, and showed that secondary particle formation from biogenic precursors dominated often over the particle sinks when the air masses travelled a distance of over 200 km. Tunved et al. (2004) investigated the south-to-north air mass transport from Aspvreten in South Sweden to Värriö in North Finland, whereas Tunved et al. (2006b) analyzed the transport to the opposite direction from the Finnish Lapland to Hyytiälä, which is located about 300 km to the north of Helsinki. According to these studies, there was a significant difference between these two transport directions on the dynamics of the measured particle size distributions: When air masses were moving to the south, the number concentration of particles in the Aitken mode was seen to grow while the mode peak diameter of the size distribution remained unaltered, whereas for the opposite direction the mode peak in the size distribution was seen to move to larger sizes, so that although the total number concentration of particles decreased, the total mass concentration grew.

An alternative approach was introduced by Tunved et al. (2006a), who classified air mass trajectories arriving at Finnish rural stations based on their transport time over the boreal forest area. By combining a large set of such trajectories, they were able to determine the “average” dynamical behavior of secondary particles formed in clean air transported from sea areas to over the forest. They found that it takes a few hours before air masses entering the boreal forest zone start to produce new particles, and that the newly-formed particles grow gradually in size in response to biogenic emissions during the atmospheric transport. The particle mass concentration was found to increase roughly linearly with the total estimated monoterpene emission into the moving air parcel, whereas the total particle number concentration appeared to saturate

between about 1000 and 2000 cm⁻³ after a couple of days of the air mass transport time.

In this manuscript, we combine the two approaches discussed above for the measurement data obtained from three stations located within a few hundred km from each other at the northern edge of the boreal forest zone. We will focus our attention on the extended summer season (April to September), which is the time period with active biogenic aerosol formation and low regional anthropogenic primary particle emissions. The principal goal of this paper is to get new insight into aerosol dynamical processes taking place in air masses transported over high northern latitudes. More specifically, we aim to address the following questions: (i) are there fundamental aerosol dynamical differences between air masses entering the different stations, or in air transported between the different station pairs?, (ii) does the west-to-east air mass transport differ from the east-to-west transport in any observable way?, (iii) how fast do particles grow effectively in size during air mass transport and how does this differ from the growth observed during nucleation events at fixed measurement sites?, and (iv) what is the net effect of aerosol source and sink processes on particle number concentrations during atmospheric transport? We hypothesize that aerosol formation and growth influence the boreal forest aerosol properties during the whole extended summer period, not just during the days with most active new particle formation, and that the net effect of these processes on the particle number size distribution is most pronounced in clean marine air masses entering the boreal forest region.

Analysis of particle size distribution changes

R. Väänänen et al.

Title Page

Abstract

Introduction

Conclusions

References

Tables

Figures



Back

Close

Full Screen / Esc

Printer-friendly Version

Interactive Discussion



2 Materials and methods

2.1 Measurements

2.1.1 Site descriptions

In this paper we compare aerosol size distribution data from three rural stations. Two of them, Värriö and Pallas, are continuous particle measurement stations and situated in Finland. They are completed with campaign data from Abisko, situated in Sweden near the border of Norway. The measurement sites are located roughly in line from west to east on latitude 67–68° N (see Fig. 1), and the distance from Abisko to Värriö is approximately 440 km.

Abisko (68.35° N, 19.05° E, 360 m a.s.l.) (see Svenningsson et al., 2008). The measurements were made at Stordalen mire 14 km east from the Abisko research station. The mire is situated between Lake Torneträsk and the Kiruna–Narvik road and railway lines in a wide east-west oriented valley. The surrounding landscape is dominated by a mix of subarctic mire, birch forest, and mountain tundra. The main chain of mountains with several peaks above 1500 m above sea level is located west from the site, and further west is the coast of the Atlantic Ocean at c. 100 km from the station.

Pallas (67.97° N, 24.12° E, 565 m a.s.l.) (see Hatakka et al., 2003). The Sammaltunturi measurements site at Pallas–Sodankylä GAW station is situated on the top of a fell about 300 m above the surrounding area. The surroundings of the station are covered by mixed boreal forest with Scots pine, spruce and birch trees, whereas the site itself is located about 100 m above the timber line. There are no significant local or regional pollution sources close to the site.

Värriö (67.77° N, 29.58° E, 390 m a.s.l.) (see Hari et al., 1994). The SMEAR (Station for Measuring Ecosystem-Atmospheric Relations) I station in Värriö is situated on a hill top and it is surrounded by an approximately 60 yr old Scots pine forest. The Värriö research station is located about 1 km south from the measurement site. The altitude of the site, 390 m a.s.l., is slightly below the timber line of the surroundings of the station,

400 m a.s.l. There are no local pollution sources close to the station. The distance to the nearest small road is 8 km and the distance to the nearest major road is 100 km. The main anthropogenic pollution sources are the mining area in Kovdor and Nickel-copper smelters Montchegorsk and Nikel located in Russia 43 km, 150 km and 190 km, respectively, from the station.

2.1.2 Instrumentations

Data were collected between 1 August 2005 and 31 December 2008. The number size distribution measurements were performed using either a Differential Mobility Particle Sizer (DMPS) or a Scanning mobility particle sizer (SMPS). Both instruments are based on particle mobility techniques, in which particles are charged and then classified according to their electrical mobility. The number density of several particle diameter bins is counted.

In Abisko an SMPS was used with a custom-built Hauke type Differential Mobility Analyzer (DMA) and TSI model 3010 Condensational Particle Counter (CPC) (Svenningsson et al., 2008). The size range of the instrument was 10–500 nm and the time resolution was 3–5 min. The inlet was placed 3.4 m/4.4 m above the surrounding mire.

In Pallas the particle size distribution data were measured using a DMPS with a Hauke-type DMA and TSI CPC model 3010 (Komppula et al., 2003). The measurement range was 7–500 nm, and the size range was scanned once in every 5.5 min. The measurement inlet was 7 m above the ground (Komppula et al., 2005).

In Värriö station a DMPS was used with two Hauke type DMAs and a TSI model 3025 CPC (Ruuskanen et al., 2003; Dal Maso et al., 2005). The size range of the measured aerosols was 3–850 nm, and the time resolution was 10 min. The inlet was situated at the height of 2 m on the wall of the measurement station.

Analysis of particle size distribution changes

R. Väänänen et al.

Title Page

Abstract

Introduction

Conclusions

References

Tables

Figures



Back

Close

Full Screen / Esc

Printer-friendly Version

Interactive Discussion



2.2 Data analysis methods

2.2.1 New particle formation events

We analyzed the particle size distributions of each day and classified the days into event, non-event, and undefined days according to the schema created by Dal Maso et al. (2005) (see also Kulmala et al., 2012). At an event day a new growing sub-25 nm particle mode that lasts for at least an hour was observed, and at an undefined day either non-growing new sub-25 nm mode or a growing > 25 nm mode was seen. If there were neither a growing nor a sub-25 nm mode, the day was classified as a non-event day. Furthermore, the event days were divided into classes Ia and Ib according to whether it was possible to calculate growth and formation rates of freshly-nucleated particles. For the class Ia events, we fitted a sum of up to three lognormal distributions to the particle number-size distribution data (Hussein et al., 2005) in order to get the geometric mean diameters of each mode. The growth and formation rates were calculated as in Dal Maso et al. (2005). The growth rate was obtained by fitting a line to the geometric mean diameters of the sub-25 nm modes during the formation burst, and the formation rate was calculated using the equation

$$J_{\text{nuc}} = \frac{dN_{\text{nuc}}}{dt} + F_{\text{coag}} + F_{\text{growth}} \quad (1)$$

where dN_{nuc}/dt is the rate of change of nucleated particle concentration, F_{coag} is the loss of particles by coagulation and F_{growth} is the rate of particles growing out of the size range. The detection limits of the DMPS or SMPS instruments varied between 3 and 10 nm, which also affected the calculated rates.

2.2.2 Aerosol dynamics over the continent

Tunved et al. (2006a) showed that the total mass concentration of submicron aerosol particles in the background air over Scandinavia is linearly proportional to the time

Analysis of particle size distribution changes

R. Väänänen et al.

Title Page

Abstract

Introduction

Conclusions

References

Tables

Figures

◀

▶

◀

▶

Back

Close

Full Screen / Esc

Printer-friendly Version

Interactive Discussion



the corresponding air mass had spent over the continent. In this work we repeated and widened this analysis to include also Abisko. We calculated and intercompared the median particle size distributions for all stations as a function of the time the corresponding air masses had spent over the continent during the last 96 h. We also calculated the apparent growth rate and the increase rates of the particle number and mass concentration and condensation sink for all the three stations considered here. In the air mass analysis we used the trajectories calculated using the HYSPLIT model (Draxler and Hess, 1998). We limited this study seasonally to the summer period between 1 April and 30 September, since the organic vapors from the biosphere are likely to be low during the winter time when the ground is covered by snow.

At each station, we calculated the hourly averages of particle size distributions, and assigned them to the corresponding over-land times calculated from the trajectories. For each of these size distributions we quantified the particle diameter that had the maximum concentration (referred to as peak diameter). Peak diameters increased as a function of the over-land time. To quantify this apparent growth, we first took all the peak diameters for each fixed over-land hour-bin, and calculated their geometric count median diameters (CMD). We used these CMD values for further analysis instead of the mean values, since for a fixed over-land time the peak diameters were lognormally distributed. Finally, we determined the apparent growth rate by fitting a line to these CMD values as a function of over-land time. For statistical reasons, only those over-land hour-bins with more than 10 size distributions were taken into account.

Similar steps, as described above, were carried out to calculate the mass accumulation rate and the condensation sink (Dal Maso et al., 2002) increase rate as a function of the over-land time. When calculating the apparent growth, our initial values were the peak diameters, but now we used the mass concentrations or condensation sink values calculated from the number size distributions. The count mean diameter values of both of these were calculated for each over-land hour-bin, and a line was fitted along them. The average density of the aerosol particles was assumed to be 1.5 g cm^{-3} (as in Tunved et al., 2006a). We concentrated our study to the largest common range of

Analysis of particle size distribution changes

R. Väänänen et al.

Title Page

Abstract

Introduction

Conclusions

References

Tables

Figures



Back

Close

Full Screen / Esc

Printer-friendly Version

Interactive Discussion



particle diameters that was measured at each of stations, namely to sizes between 10 and 450 nm, to make the results intercomparable.

2.2.3 Aerosol transport between stations

Particle size distribution data from several measurement stations combined with the calculated air mass trajectory information allowed us to study regionally the dynamical changes of aerosol particle populations. For this, we focused on the air masses that had travelled over two stations, and then compared the aerosol properties between the different station pairs. Each station pair had an upwind and a downwind station.

When studying the aerosol dynamics, the initial states need to be comparable. For this, we clustered the particle size distributions measured at the upwind station to obtain a set of different initial states. Kmeans clustering algorithm from Matlab Optimization toolbox (MathWorks Inc., 2011) was used for the task. The algorithm groups the data into k clusters so that measure between cluster centrum and its members are minimized. In other words it tries to find subsets from the data that are internally similar to each other, in our case similar aerosol size distributions. Measured aerosol size distributions were mapped into logarithmically spaced size bin basis and concentrations normalized by the size bin ($dN/d\log D_p$, where dN is number concentration is a size bin and $d\log D_p$ is logarithm of the size bin). Now we could calculate the squared Euclidian measure between two size distributions. Kmeans method with squared Euclidian measure as a measure had been shown to work best when comparing several particle size distribution clustering algorithms (Beddows et al., 2009). However, our method differed from the normalization by Beddows et al. (2009), who had normalized the vector lengths. We did not do this, since we were also interested in the aerosol loading, not only the shapes of the distributions.

One should note that the basis vectors used in our clustering algorithm were chosen in a practical, not in a mathematical way, so the basis vectors are not are not a normalized Euclidean basis set, although we use Euclidean measure. Our aim was

Analysis of particle size distribution changes

R. Väänänen et al.

Title Page

Abstract

Introduction

Conclusions

References

Tables

Figures

◀

▶

◀

▶

Back

Close

Full Screen / Esc

Printer-friendly Version

Interactive Discussion



to divide the size distributions into groups with different physical properties, and the method suited for that.

Typically, our procedure resulted in 3–6 clusters per site. Of these, because of the low generalization, clusters with less than 30 size distributions were disregarded. Each of the studied clusters was linked to a set of size distributions at the downwind station via the trajectories. The statistical size distributions (mean, and 16th and 83th percentiles) for each cluster were calculated and plotted at both the upwind and downwind station. Furthermore, we fitted a sum of lognormal distributions to the mean size distributions and analyzed the dynamics of the particle modes.

We chose the trajectories that passed several measurement sites in the following way. First, the 96 h HYSPLIT backward trajectories that arrived at each station were calculated once per hour, each with a time resolution of one hour. We increased the resolution of each trajectory to ten minutes by interpolating the paths. We defined that an arriving trajectory had passed another site if it had gone through a circle with a radius of 25 km centered to the other site. Such a radius was based on the uncertainty of the trajectories, which can be of order of 10–30 % of the distance the trajectory had proceeded (Stohl, 1998). This means that when the distance from Pallas to Värriö or from Abisko to Pallas is about 200 km, the location error can be tens of kilometers. The terrain below the air mass affects the amount of the organic vapors available. We reduced the effects of different land use by restricting the trajectory paths to be between the latitudes of 67.1–69.0° N.

3 Results and discussion

Our data covered the measured size distributions in the three stations between August 2005 and December 2008. The gaps in the dataset limit the intercomparison of the new particle formation analysis (Fig. 2). The most complete dataset was from Värriö, most gaps were in the Abisko data set which was derived during a number of shorter measurement campaigns. The fractions of days without data during the whole time

Analysis of particle size distribution changes

R. Väänänen et al.

Title Page

Abstract

Introduction

Conclusions

References

Tables

Figures



Back

Close

Full Screen / Esc

Printer-friendly Version

Interactive Discussion



Analysis of particle size distribution changes

R. Väänänen et al.

Title Page

Abstract

Introduction

Conclusions

References

Tables

Figures

◀

▶

◀

▶

Back

Close

Full Screen / Esc

Printer-friendly Version

Interactive Discussion



period were 52 %, 13 %, and 6 % for Abisko, Pallas and Värriö, respectively. The periods when there were data from all the measurement stations were biased to summer and autumn. Since there were no data from most of the winter days at Abisko, the fraction of the event days compared to all analyzed (Ev/A) or classified (either event or non-event) (Ev/Cl) days in Abisko cannot be directly compared to those at Pallas or Värriö. When comparing Pallas and Värriö, we found that there was a slightly higher fraction of event days at Pallas (Fig. 3 and Table 1).

When comparing our results to studies containing longer time series, overall the differences were quite small and they were probably within normal interannual variation. In a study containing seven years from Värriö and five years from Pallas (Dal Maso et al., 2007), both Ev/A and Ev/Cl fractions were very similar to ours in Pallas and slightly higher in Värriö (19 % EV/A or 27 % Ev/Cl). Vehkamäki et al. (2004) found in a five-year study of Värriö lower fractions (monthly Ev/A varied between 3 and more than 20 %), but applied a slightly different classification from ours, which might cause some differences. In an 11 yr study of Pallas, the value of Ev/A varied between 6 and 27 % during different months (Asmi et al., 2011).

The particle formation rates were calculated from the cut-off size of each instrument, which varied between 3 and 10 nm, which made easier to compare the results to the previous studies (Table 2). The mean formation rates were almost equal at all the sites ($0.1 \text{ cm}^{-3} \text{ s}^{-1}$) and confirm previously published results (Vehkamäki et al., 2004; Dal Maso et al., 2007; Asmi et al., 2011). The mean growth rate of particles during the new particle formation events in Abisko exceeded the growth rates in Pallas and Värriö.

3.1 Evolution of the particle properties over the continent

It has been shown for both Pallas and Värriö that, on average, the particle size and the accumulated particle mass concentration grows as a function of time that the corresponding air mass has spent over the land (Asmi et al., 2011; Tunved et al., 2006b). We extended this analysis to include Abisko. We considered the summertime trajectories ending to these stations and calculated the median particle size distributions as a

function of the time the air mass had spent over land (Fig. 4), as well as the mode peak diameter, the total particle number concentration, mass concentration, and condensation sink (Fig. 5).

An air mass originating from the sea and arriving at the continental areas was assumed to be relatively clean. Observed particle number size distributions (Fig. 4) and low total aerosol number concentrations (Fig. 5c) associated with the short over-land times support this assumption. With short over-land times, the particle size distribution in all stations had a bi-modal structure with mode peaks at 30–40 nm and 130–170 nm. This feature suits well with measured marine aerosol number size distributions (Covert et al., 1996; Koponen et al., 2002; Heintzenberg et al., 2004; O'Dowd et al., 2004).

When the air mass travelled over the land, the formation and growth of aerosol particles could be observed as the particle number concentration increased and the mean diameter of the Aitken mode grew. The number concentrations increased rapidly until over-land times of around 30–40 h (Fig. 5c). After that, there was a small drop in the number concentrations and slow saturation towards levels of 900–1100 cm⁻³. This indicates that by then the formation of new particles as the main feature had been overtaken either by vapors condensing or by small clusters coagulating onto the larger particles. By contrast to the number concentration, particle mode diameter, accumulated mass concentration and condensation sink increased during the entire 96 h time period (Fig. 5a, b, d). The condensation sink values corresponding to the 30–40 h land-over-time were between $0.8 \times 10^{-3} \text{ s}^{-1}$ and $1.2 \times 10^{-3} \text{ s}^{-1}$.

The median particle size distributions were found to have similar structures at all the stations. For over-land times less than 40–50 h, the size distributions were bimodal. The mode with the smaller particle diameter started at around 20–30 nm and grew as a function of time, whereas the second mode with particle diameters of around 100–200 nm remained more stationary. When comparing the means of these size distributions for 10–20 h over-land times (blue lines in Fig. 4d), we see that the shape of the size distributions was similar between the stations, but Abisko had the highest number concentration of Aitken mode particles. For over-land times of 30–40 h (black

Analysis of particle size distribution changes

R. Väänänen et al.

Title Page

Abstract

Introduction

Conclusions

References

Tables

Figures

◀

▶

◀

▶

Back

Close

Full Screen / Esc

Printer-friendly Version

Interactive Discussion



lines in Fig. 4d), Abisko and Pallas had similar size distributions and Värriö had the highest Aitken mode particle number concentrations. Comparing the size distributions (Fig. 4a–c) and calculated number concentrations and mode diameters (Fig. 5), one can see that all the stations had a time period when the number concentration dropped although the particle mode diameter was growing. For Abisko and Pallas this took place between 30 and 45 h and for Värriö between 40 and 55 h. For over-land times of 60–70 h, the size distributions (red lines in Fig. 4d) at all stations were relatively similar.

In order to compare the growth of the particles, we calculated the apparent increase rates with error limits for the mode peak diameter, mass accumulation and condensation sink using the method explained in Sect. 2.2.2 (Table 3). One should note that the error limits were based on a mathematical line fitting, which omits the physical uncertainty in the measurements, the inaccuracy of the method itself and the pre-assumptions made of the data (e.g. which time interval was used when calculating the rates), which are complicated to access. Thus the reported errors should be considered as lower-limit estimates for the errors.

The apparent particle growth rates when air masses were passing over the land were relatively similar for all the stations, between 0.55 and 0.72 nm h⁻¹. As a comparison, the medians of the particle growth rates during the NPF events were about 3–6 times higher than the apparent growth rates obtained when taking into account all the days regardless of their classification. The main reason for these differences was that, by definition, during an event day the growth needs to be considerable. And also the viewpoint is different: growth rates obtained from NPF events measure real particle growth, whereas the apparent growth as a function of the over-land time is a statistical quantity that may include aerosol dynamic processes beyond the particle growth. Compared to Värriö, Pallas had both larger growth rates during the NPF events and also larger apparent growth rates. Abisko had the lowest apparent growth rates but the highest median growth rate during NPF events.

To ensure that the apparent particle growth was not caused only by averaging the NPF events over all days, we calculated a separate apparent growth rate using data

Analysis of particle size distribution changes

R. Väänänen et al.

Title Page

Abstract

Introduction

Conclusions

References

Tables

Figures

◀

▶

◀

▶

Back

Close

Full Screen / Esc

Printer-friendly Version

Interactive Discussion



from the non-event days only. As a result, no significant difference to all-data results was seen.

In Tunved et al. (2006a), the average integrated observed particle mass for Pallas and Värriö was calculated to increase by $0.014 \mu\text{g m}^{-3} \text{h}^{-1}$ with the time the corresponding air mass had spent over the continent. In our analysis we obtained similar values despite the different datasets used. The integrated particle mass concentration increase rates in our study were between 0.015 and $0.023 \mu\text{g m}^{-3} \text{h}^{-1}$. The over-land times used here to calculate the slopes was chosen to be below 50 h because a linear fit suited best for such a time window. If the upper limit was chosen to be 80 h, slightly larger (between 0.020 and $0.027 \mu\text{g m}^{-3} \text{h}^{-1}$) slopes were obtained, but the fitting was worse. The condensation sink was found increase linearly with over-land-time at all stations. The corresponding increase rates were between 0.020 and $0.030 \text{s}^{-1} \text{h}^{-1}$. Värriö had the highest value in line with the other variables: Värriö had also the highest apparent growth rate, mass accumulation rate and particle number concentration after its saturation.

When looking at the apparent growth and accumulated particle mass increase, we found some differences between the stations. Both these rates were the lowest for Abisko. However, the differences between the values were not large, and particularly the accumulated mass increase rates for Pallas and Abisko were close to each others.

The histogram of the times that the trajectories had spent over land peaked at 8 h for Abisko and at around 20 h for Pallas and Värriö (Fig. 6a), reflecting the relative distances of these stations from the ocean and the prevailing westerly winds. For Pallas and Värriö, the trajectories corresponding to NPF event days peaked at around 20–25 h on-land times, slightly earlier in Pallas (Fig. 6b). This supports the principal idea that particle nucleation occurs easier in fresh air coming from the ocean, while the transport time need to be sufficient for enough condensable gases to be formed. However, for Abisko the distribution was relatively flat with a higher NPF fraction already at smaller over-land times compared to Pallas and Värriö. The reason for the observed differences between Abisko compared with Pallas and Värriö cannot be explained by the

Analysis of particle size distribution changes

R. Väänänen et al.

[Title Page](#)[Abstract](#)[Introduction](#)[Conclusions](#)[References](#)[Tables](#)[Figures](#)[Back](#)[Close](#)[Full Screen / Esc](#)[Printer-friendly Version](#)[Interactive Discussion](#)

differences in the values of the condensation sink (Fig. 5d). Moreover, for the extended summer season (April to September during 2005–2007), there was no significant difference between the stations regarding their climatology (Fig. 7). Therefore, the reason for the earlier onset of nucleation in Abisko compared to Pallas and Värriö must be due to other factors. Compared to Pallas and Värriö, Abisko has very distinct geographical features as it is located on the lee side of the Scandinavian mountains and thus affected by air descending the mountain range, whereas Pallas and Värriö are both located on top of a hill. The Scandinavian mountains generate very often (Jiang et al., 2004; Schroeder et al., 2009) standing atmospheric gravity waves (Nappo, 2002; Scorer, 1949) on their lee side. In this kind of situation, we speculate that the lee-side boundary layer is compressed, so there would be more condensable gases per unit volume of air and the amount of vapors that are required for new particle formation is accumulated faster. This would be the only major difference between the stations we could find that might be able to increase the probability of nucleation already at an earlier stage (Fig. 7). The faster nucleation onset in Abisko was also seen from the median size distributions (Fig. 4a–c): the time when particle number concentrations in the Aitken mode increased significantly was around 7 h for Abisko, 15 h for Pallas and 20 h for Värriö.

One should note that even though the average climate was fairly similar, the average meteorological conditions related to the short over-land times were different between the stations: for the same over-land time, the longer distance from the ocean to Pallas or Värriö than to Abisko indicates higher wind speeds, which is likely to be connected to a lower pressure and thus different rain and radiation profiles. This, in turn, affects the event day probability.

3.2 Aerosol dynamics between measurement stations

Three measurement sites located in a row of the total distance of 440 km offered the possibility to examine the dynamical properties of aerosols when they are transported by air masses between sites. To do so, the particle number size distributions at the

Analysis of particle size distribution changes

R. Väänänen et al.

Title Page

Abstract

Introduction

Conclusions

References

Tables

Figures



Back

Close

Full Screen / Esc

Printer-friendly Version

Interactive Discussion



upwind station need to be known. To standardize the starting situations, we first clustered the size distributions at the upwind station separately for both summer and winter seasons, and then the changes of each of these clusters were analyzed.

The changes of the size distributions of each cluster at the upwind and downwind station show the average evolution during the transport (Figs. 8 and 9). We fitted a sum of lognormal size distributions to the mean size distributions of both stations in each pair to identify the changes in aerosol modes. The resulting peak diameters of these modes and their changes, as well as the mode concentrations and their changes, are listed for summer and winter periods in Tables 4 and 5, respectively. Since our purpose was to use clusters as being representative for general patterns rather than just single cases, all clusters with less than 30 size distribution elements at both ends were discarded. Next we will analyze both air mass transport directions and all the station pairs along these transport routes.

3.2.1 Abisko-Pallas

When clustering the size distributions at Abisko, related to air masses in direction towards Pallas, the best clustering was obtained with five clusters for the summer period and with three clusters for the winter period. During the summer two of the clusters had more than 30 elements, whereas during winter only one cluster had enough elements.

The largest cluster at Abisko had a bimodal structure with almost the same mode peak diameters in both seasons, but in the summer the particle concentration of the Aitken mode was almost double compared to the winter case. In both seasons, the Aitken-mode particle number concentration increased during the air mass transport, whereas the accumulation-mode number concentration remained roughly unaltered. During the summer, the peak diameter of the Aitken mode shifted from 29 nm up to 48 in 15 h, which corresponds to a rate of 1.3 nm h^{-1} , whereas during winter practically no shift was seen. The absence of changes during winter compared to the pronounced shift in the distribution in the growing season is most likely connected to the condensation of organic compounds formed from soil and vegetation emissions. The

Analysis of particle size distribution changes

R. Väänänen et al.

Title Page

Abstract

Introduction

Conclusions

References

Tables

Figures

◀

▶

◀

▶

Back

Close

Full Screen / Esc

Printer-friendly Version

Interactive Discussion



concentrations of the combined nucleation and Aitken-mode particles increased with a rate of $0.01 \text{ cm}^{-3} \text{ s}^{-1}$ during the summer, and the corresponding increase during the winter was around one third of this. In both seasons, the accumulation mode of the first cluster had a larger mode peak diameter but a smaller concentration in Pallas than at Abisko.

In summer at Abisko, the most dominant mode of the second cluster was the accumulation mode with a peak diameter of 148 nm. After arriving at Pallas, this mode peaked at about the same size as it did in Abisko, and the particle concentration of that mode had increased slightly with a rate of $0.004 \text{ cm}^{-3} \text{ s}^{-1}$.

3.2.2 Pallas-Värriö

Particle number size distributions observed at Pallas, when considering trajectories in direction to Värriö, clustered to four sets in the summer and to three sets in the winter season, of which two in both cases had enough members for a further analysis. For the more dominant cluster, during the summer, the Aitken mode shifted towards larger particles (0.6 nm h^{-1}) and its concentration increased ($0.02 \text{ cm}^{-3} \text{ s}^{-1}$). In winter, the mode peak diameter of Aitken-mode particles shifted with a high rate of 2.1 nm h^{-1} , but the concentration increase was low with a rate of $0.004 \text{ cm}^{-3} \text{ s}^{-1}$. In summer, the accumulation mode shifted rapidly towards larger particles (3.3 nm h^{-1}) and its concentration increased slightly ($0.004 \text{ cm}^{-3} \text{ s}^{-1}$). During wintertime, the accumulation mode was very weak already in Pallas and did not change much. In summer, the general modal dynamics was quite similar to that associated with the Abisko-Pallas transport route.

In both seasons, the accumulation mode dominated the second dominant cluster at Pallas and the Aitken mode was also present. During the summer period, the number concentrations of the accumulation mode decreased and those in the Aitken mode increased, but the mode peak diameters of both modes remained unchanged. During the winter period, the peak diameters of both modes increased rapidly (1.7 nm h^{-1} for

Analysis of particle size distribution changes

R. Väänänen et al.

Title Page

Abstract

Introduction

Conclusions

References

Tables

Figures

◀

▶

◀

▶

Back

Close

Full Screen / Esc

Printer-friendly Version

Interactive Discussion



the Aitken mode and 2.7 nm h^{-1} for the accumulation mode), and also the concentration of accumulation mode increased slightly.

3.2.3 Pallas-Abisko

The Pallas-Abisko air transport route had the least number of paired size distributions and the clustering could be done for the summer season only. Also, although the summer data were best fitted using four clusters, only one of them had over 30 data-pairs. As a result, the conclusions from this analysis are not as firm as from the other transport routes.

The size distribution at Pallas for the only cluster had a low total concentration and trimodal structure with mode peak diameters of 22 nm, 63 nm and, 169 nm. On average, these peak diameters remained relatively unchanged when the air masses travelled to Abisko, and the total concentrations on all size ranges increased. For all the modes, particle number concentrations increased at the rate of $0.002 \text{ cm}^{-3} \text{ s}^{-1}$.

3.2.4 Värriö-Pallas

The Värriö-Pallas path included the highest diversity of all observed size distributions. The clustering procedure resulted in six sets of distributions for the summer and four sets for the winter. In both seasons, the two largest clusters had over 30 elements and were chosen to be studied in more detail.

During both summer and winter, the most dominant cluster had a bimodal structure and no significant change in the total particle number concentration was seen during the transport. During the summer, this zero total concentration change was achieved by a small increase of Aitken-mode particle concentration while the accumulation-mode particles decreased. The total particle number concentrations were slightly higher during the summer than winter.

For the second dominant cluster, the accumulation mode was the dominant one at Pallas in both summer and winter. During the atmospheric transport, the total particle

Analysis of particle size distribution changes

R. Väänänen et al.

Title Page

Abstract

Introduction

Conclusions

References

Tables

Figures



Back

Close

Full Screen / Esc

Printer-friendly Version

Interactive Discussion



**Analysis of particle
size distribution
changes**

R. Väänänen et al.

Title Page

Abstract

Introduction

Conclusions

References

Tables

Figures

◀

▶

◀

▶

Back

Close

Full Screen / Esc

Printer-friendly Version

Interactive Discussion



the formation of new particles. Secondly, the wind direction was associated with different meteorological conditions. We calculated the relative humidity along the trajectories between the measurement station pairs. For the summer time, the median values of relative humidity for each cluster associated with the west-to-east paths were between 72 and 78 %, whereas for the opposite paths they were between 81 and 85 %. The higher relative humidity values have been connected to lower NPF probabilities e.g. at Pallas (Asmi et al., 2011).

During both seasons and wind directions, the second most frequent clusters included a strong accumulation mode at the upwind station, and the same mode dominated also in the downwind station. This was presumable because accumulation-mode particles have the longest lifetime in atmosphere. The highest decreases in the accumulation-mode concentration were seen between Pallas and Värriö for both directions during the summer time.

The observed shifts in the place of the Aitken mode were around of 1 nm h^{-1} during the summer period. This was close to the value of the apparent growth rates obtained when studying the particle evolution when they travel over land. Again this was about one third of the average growth rate observed during NPF events. The increase rates of the Aitken mode particles were up to $0.02 \text{ cm}^{-3} \text{ s}^{-1}$. When comparing it to the average formation rates during the NPF event, we saw that the latter were five times larger. These differences reflect the choice of the data behind the values and stress that the growth and formation rates observed only during the most obvious nucleation days can give misleading numbers of the changes of the total aerosol population.

4 Summary and conclusions

Three different approaches for the nucleation and growth of aerosol particles in Northern Scandinavia gave mutually supportive information on the evolution of the aerosol population. When studying the average air masses arriving at the different stations, we found that the apparent increase rates of particle mode diameters, accumulated mass

during new particle formation events. This indicates that the condensational growth has an important effect in the regional-scale air masses also when the evident nucleation, i.e. “banana curve”, is not observed.

During the atmospheric transport, the net effect of the source and sink processes on the particle number concentration depends on the initial aerosol population and its time evolution. The new particle formation was seen to increase particle number concentrations for over-land times up to 30–40 h or, alternatively, as long as the diameter of the Aitken mode particles remained below about 40–50 nm. After that the particle number concentration saturated, which means that new particle formation was balanced by coagulation and other sink processes. The net accumulation of secondary mass on newly-formed and pre-existing aerosol particles seemed to continue for at least 4 days of over-land transport time.

Acknowledgements. The financial support by the Academy of Finland Centre of Excellence program (project no. 1118615) and the Nordic Centre of Excellence CRAICC (CRyosphere-Atmosphere Interactions in Changing Climate) are gratefully acknowledged.

References

- Asmi, E., Kivekäs, N., Kerminen, V.-M., Komppula, M., Hyvärinen, A.-P., Hatakka, J., Viisanen, Y., and Lihavainen, H.: Secondary new particle formation in Northern Finland Pallas site between the years 2000 and 2010, *Atmos. Chem. Phys.*, 11, 12959–12972, doi:10.5194/acp-11-12959-2011, 2011.
- Beddows, D. C. S., Dall’Osto, M., and Harrison, R. M.: Cluster analysis of rural, urban, and curbside atmospheric particle size data, *Environ. Sci. Technol.*, 43, 4694–4700, doi:10.1021/es803121t, 2009.
- Covert, D. S., Wiedensohler, A., Aalto, P., Heintzenberg, J., McMurry, P. H., and Leck, C.: Aerosol number size distributions from 3 to 500 nm diameter in the arctic marine boundary layer during summer and autumn, *Tellus B*, 48, 197–212, doi:10.1034/j.1600-0889.1996.t01-1-00005.x, 1996.

Analysis of particle size distribution changes

R. Väänänen et al.

Title Page

Abstract

Introduction

Conclusions

References

Tables

Figures

◀

▶

◀

▶

Back

Close

Full Screen / Esc

Printer-friendly Version

Interactive Discussion



**Analysis of particle
size distribution
changes**

R. Väänänen et al.

Title Page

Abstract

Introduction

Conclusions

References

Tables

Figures

◀

▶

◀

▶

Back

Close

Full Screen / Esc

Printer-friendly Version

Interactive Discussion



Dal Maso, M., Kulmala, M., Lehtinen, K., Mäkelä, J., Aalto, P., and O'Dowd, C.: Condensation and coagulation sinks and formation of nucleation mode particles in coastal and boreal forest boundary layers, *J. Geophys. Res.*, 107, 8097, doi:10.1029/2001JD001053, 2002.

Dal Maso, M., Kulmala, M., Riipinen, I., Wagner, R., Hussein, T., Aalto, P. P., and Lehtinen, K. E. J.: Formation and growth of fresh atmospheric aerosols: eight years of aerosol size distribution data from SMEAR II, Hyytiälä, Finland, *Boreal Env. Res.*, 10, 323–336, 2005.

Dal Maso, M., Sogacheva, L., Aalto, P. P., Riipinen, I., Komppula, M., Tunved, P., Korhonen, L., Suur-Uski, V., Hirsikko, A., Kurtén, T., Kerminen, V.-M., Lihavainen, H., Viisanen, Y., Hansson, H., and Kulmala, M.: Aerosol size distribution measurements at four Nordic field stations: identification, analysis and trajectory analysis of new particle formation bursts, *Tellus B*, 59, 350–361, doi:10.1111/j.1600-0889.2007.00267.x, 2007.

Draxler, R. R. and Hess, G.: An overview of the HYSPLIT_4 modelling system for trajectories, dispersion, and deposition, *Aust. Meteorol. Mag.*, 47, 295–308, 1998.

Flanner, M. G., Zender, C. S., Hess, P. G., Mahowald, N. M., Painter, T. H., Ramanathan, V., and Rasch, P. J.: Springtime warming and reduced snow cover from carbonaceous particles, *Atmos. Chem. Phys.*, 9, 2481–2497, doi:10.5194/acp-9-2481-2009, 2009.

Hari, P., Kulmala, M., Pohja, T., Lahti, T., Siivola, E., Palva, L., Aalto, P., Hämeri, K., Vesala, T., and Luoma, S.: Air pollution in eastern Lapland: challenge for an environmental measurement station, *Silva Fennica*, 28, 29–39, 1994.

Hatakka, J., Aalto, T., Aaltonen, V., Aurela, M., Hakola, H., Komppula, M., Laurila, T., Lihavainen, H., Paatero, J., and Salminen, K.: Overview of the atmospheric research activities and results at Pallas GAW station, *Boreal Env. Res.*, 8, 365–383, 2003.

Heintzenberg, J., Birmili, W., Wiedensohler, A., Nowak, A., and Tuch, T.: Structure, variability and persistence of the submicrometre marine aerosol, *Tellus B*, 56, 357–367, doi:10.1111/j.1600-0889.2004.00115.x, 2004.

Hussein, T., Dal Maso, M., Petäjä, T., Koponen, I.K., Paatero, P., Aalto, P.P., Hämeri, K., and Kulmala, M.: Evaluation of an automatic algorithm for fitting the particle number size distribution, *Boreal Env. Res.*, 10, 337–355, 2005.

Jiang, J. H., Eckermann, S. D., Wu, D. L., and Ma, J.: A search for mountain waves in MLS stratospheric limb radiances from the winter Northern Hemisphere: Data analysis and global mountain wave modeling, *J. Geophys. Res.*, 109, D03107, doi:10.1029/2003JD003974, 2004.

**Analysis of particle
size distribution
changes**

R. Väänänen et al.

Title Page

Abstract

Introduction

Conclusions

References

Tables

Figures

◀

▶

◀

▶

Back

Close

Full Screen / Esc

Printer-friendly Version

Interactive Discussion



- Kerminen, V.-M., Lihavainen, H., Komppula, M., Viisanen, Y., and Kulmala, M.: Direct observational evidence linking atmospheric aerosol formation and cloud droplet activation, *Geophys. Res. Lett.*, 32, L14803, doi:10.1029/2005GL023130, 2005.
- Komppula, M., Lihavainen, H., Hatakka, J., Paatero, J., Aalto, P., Kulmala, M., and Viisanen, Y.: Observations of new particle formation and size distributions at two different heights and surroundings in subarctic area in northern Finland, *J. Geophys. Res.*, 108, 4295, doi:10.1029/2002JD002939, 2003.
- Komppula, M., Lihavainen, H., Kerminen, V.-M., Kulmala, M., and Viisanen, Y.: Measurements of cloud droplet activation of aerosol particles at a clean subarctic background site, *J. Geophys. Res.*, 110, D06204, doi:10.1029/2004JD005200, 2005.
- Komppula, M., Sihto, S.-L., Korhonen, H., Lihavainen, H., Kerminen, V.-M., Kulmala, M., and Viisanen, Y.: New particle formation in air mass transported between two measurement sites in Northern Finland, *Atmos. Chem. Phys.*, 6, 2811–2824, doi:10.5194/acp-6-2811-2006, 2006.
- Koponen, I. K., Virkkula, A., Hillamo, R., Kerminen, V.-M., and Kulmala, M.: Number size distributions and concentrations of marine aerosols: Observations during a cruise between the English Channel and the coast of Antarctica, *J. Geophys. Res.*, 107, 4753, doi:10.1029/2002JD002533, 2002.
- Kulmala, M., Suni, T., Lehtinen, K. E. J., Dal Maso, M., Boy, M., Reissell, A., Rannik, Ü., Aalto, P., Keronen, P., Hakola, H., Bäck, J., Hoffmann, T., Vesala, T., and Hari, P.: A new feedback mechanism linking forests, aerosols, and climate, *Atmos. Chem. Phys.*, 4, 557–562, doi:10.5194/acp-4-557-2004, 2004a.
- Kulmala, M., Vehkamäki, H., Petäjä, T., Dal Maso, M., Lauri, A., Kerminen, V.-M., Birmili, W., and McMurry, P. H.: Formation and growth rates of ultrafine atmospheric particles: a review of observations, *J. Aerosol Sci.*, 35, 143–176, doi:10.1016/j.jaerosci.2003.10.003, 2004b.
- Kulmala, M., Alekseychik, P., Paramonov, M., Laurila, T., Asmi, E., Arneth, A., Zilitinkevich, S., and Kerminen, V.-M.: On measurements of aerosol particles and greenhouse gases in Siberia and future research needs, *Boreal Env. Res.*, 16, 337–362, 2011.
- Kulmala, M., Petäjä, T., Nieminen, T., Sipilä, M., Manninen, H. E., Lehtipalo, K., Dal Maso, M., Aalto, P. P., Junninen, H., and Paasonen, P.: Measurement of the nucleation of atmospheric aerosol particles, *Nature Protoc.*, 7, 1651–1667, doi:10.1038/nprot.2012.091, 2012.
- Law, K. S. and Stohl, A.: Arctic Air Pollution: Origins and Impacts, *Science*, 315, 1537–1540, doi:10.1126/science.1137695, 2007.

Analysis of particle size distribution changes

R. Väänänen et al.

Title Page

Abstract

Introduction

Conclusions

References

Tables

Figures

◀

▶

◀

▶

Back

Close

Full Screen / Esc

Printer-friendly Version

Interactive Discussion



- Lihavainen, H., Kerminen, V.-M., Tunved, P., Aaltonen, V., Arola, A., Hatakka, J., Hyvärinen, A., and Viisanen, Y.: Observational signature of the direct radiative effect by natural boreal forest aerosols and its relation to the corresponding first indirect effect, *J. Geophys. Res.*, 114, D20206, doi:10.1029/2009JD012078, 2009.
- 5 Lu, J. and Cai, M.: Quantifying contributions to polar warming amplification in an idealized coupled general circulation model, *Clim. Dyn.*, 34, 669–687, doi:10.1007/s00382-009-0673-x, 2010.
- MathWorks Inc., *Matlab Documentation Center: Kmeans clustering* [Homepage of Mathworks], [Online], available at: <http://www.mathworks.se/help/stats/kmeans.html> [2012, 11/17], 2012.
- 10 Nappo, C. J.: An introduction to atmospheric gravity waves, Academic Press, San Diego, California, USA, 47–80, 2002.
- O’Dowd, C. D., Facchini, M. C., Cavalli, F., Ceburnis, D., Mircea, M., Decesari, S., Fuzzi, S., Yoon, Y. J., and Putaud, J. P.: Biogenically driven organic contribution to marine aerosol, *Nature*, 431, 676–680, doi:10.1038/nature02959, 2004.
- 15 Ruuskanen, T. M., Reissell, A., Keronen, P., Aalto, P. P., Laakso, L., Gronholm, T., Hari, P., and Kulmala, M.: Atmospheric trace gas and aerosol particle concentration measurements in Eastern Lapland, Finland 1992–2001, *Boreal Env. Res.*, 8, 335–350, 2003.
- Schroeder, S., Preusse, P., Ern, M., and Riese, M.: Gravity waves resolved in ECMWF and measured by SABER, *Geophys. Res. Lett.*, 36, L10805, doi:10.1029/2008GL037054, 2009.
- 20 Scorer, R. S.: Theory of waves in the lee of mountains, *Q. J. Roy. Meteorol. Soc.*, 75, 41–56, doi:10.1002/qj.49707532308, 1949.
- Screen, J., Deser, C., and Simmonds, I.: Local and remote controls on observed Arctic warming, *Geophys. Res. Lett.*, 39, L10709, doi:10.1029/2012GL051598, 2012.
- Shindell, D. and Faluvegi, G.: Climate response to regional radiative forcing during the twentieth century, *Nature Geosci.*, 2, 294–300, doi:10.1038/ngeo473, 2009.
- 25 Sihto, S.-L., Mikkilä, J., Vanhanen, J., Ehn, M., Liao, L., Lehtipalo, K., Aalto, P. P., Duplissy, J., Petäjä, T., Kerminen, V.-M., Boy, M., and Kulmala, M.: Seasonal variation of CCN concentrations and aerosol activation properties in boreal forest, *Atmos. Chem. Phys.*, 11, 13269–13285, doi:10.5194/acp-11-13269-2011, 2011.
- 30 Sogacheva, L., Dal Maso, M., Kerminen, V.-M., and Kulmala, M.: Probability of nucleation events and aerosol particle concentration in different air mass types arriving at Hyytiälä, southern Finland, based on back trajectories analysis, *Boreal Env. Res.*, 10, 479–491, 2005.

**Analysis of particle
size distribution
changes**

R. Väänänen et al.

Title Page

Abstract

Introduction

Conclusions

References

Tables

Figures

◀

▶

◀

▶

Back

Close

Full Screen / Esc

Printer-friendly Version

Interactive Discussion



- Spracklen, D. V., Bonn, B., and Carslaw, K.S.: Boreal forests, aerosols and the impacts on clouds and climate, *Phil. T. R. Soc. A.*, 366, 4613–4626, doi:10.1098/rsta.2008.0201, 2008.
- Spracklen, D. V., Carslaw, K. S., Pöschl, U., Rap, A., and Forster, P. M.: Global cloud condensation nuclei influenced by carbonaceous combustion aerosol, *Atmos. Chem. Phys.*, 11, 9067–9087, doi:10.5194/acp-11-9067-2011, 2011.
- 5 Stohl, A.: Computation, accuracy and applications of trajectories – A review and bibliography, *Atmos. Environ.*, 32, 947–966, doi:/10.1016/S1352-2310(97)00457-3, 1998.
- Svenningsson, B., Arneth, A., Hayward, S., Holst, T., Massling, A., Swietlicki, E., Hirsikko, A., Junninen, H., Riipinen, I., and Vana, M.: Aerosol particle formation events and analysis of high growth rates observed above a subarctic wetland–forest mosaic, *Tellus B*, 60, 353–364, doi:10.1111/j.1600-0889.2008.00351.x, 2008.
- 10 Tunved, P., Korhonen, H., Ström, J., Hansson, H.-C., Lehtinen, K. E. J., and Kulmala, M.: A pseudo-Lagrangian model study of the size distribution properties over Scandinavia: transport from Aspveeten to Värriö, *Atmos. Chem. Phys. Discuss.*, 4, 7757–7794, doi:10.5194/acpd-4-7757-2004, 2004.
- Tunved, P., Hansson, H. C., Kerminen, V.-M., Ström, J., Maso, M. D., Lihavainen, H., Viisanen, Y., Aalto, P., Komppula, M., and Kulmala, M.: High natural aerosol loading over boreal forests, *Science*, 312, 261, doi:10.1126/science.1123052, 2006a.
- Tunved, P., Korhonen, H., Ström, J., Hansson, H. C., Lehtinen, K., and Kulmala, M.: Is nucleation capable of explaining observed aerosol integral number increase during southerly transport over Scandinavia?, *Tellus B*, 58, 129–140, 2006b.
- 20 Tunved, P., Ström, J., Kulmala, M., Kerminen, V.-M., Dal Maso, M., Svenningsson, B., Lunder, C., and Hansson, H. C.: The natural aerosol over northern Europe and its relation to anthropogenic emissions – implications of important climate feedbacks, *Tellus B*, 60, 473–484, doi:10.1111/j.1600-0889.2008.00363.x, 2008.
- Vehkamäki, H., Dal Maso, M., Hussein, T., Flanagan, R., Hyvärinen, A., Lauros, J., Merikanto, P., Mönkkönen, M., Pihlatie, K., Salminen, K., Sogacheva, L., Thum, T., Ruuskanen, T. M., Keronen, P., Aalto, P. P., Hari, P., Lehtinen, K. E. J., Rannik, Ü., and Kulmala, M.: Atmospheric particle formation events at Värriö measurement station in Finnish Lapland 1998–2002, *Atmos. Chem. Phys.*, 4, 2015–2023, doi:10.5194/acp-4-2015-2004, 2004.
- 30

Analysis of particle size distribution changes

R. Väänänen et al.

[Title Page](#)[Abstract](#)[Introduction](#)[Conclusions](#)[References](#)[Tables](#)[Figures](#)[◀](#)[▶](#)[◀](#)[▶](#)[Back](#)[Close](#)[Full Screen / Esc](#)[Printer-friendly Version](#)[Interactive Discussion](#)

Table 1. Fraction of NPF event days compared to all analyzed days with data (Ev/A) or to days which are classified either to event or non-event days (Ev/CI). Data from Abisko was from campaigns (most data from the winters 2005–2006 and 2006–2007 are missing), and it thus cannot be compared to the values of Pallas and Värriö.

	Ev/A (%)	Ev/CI (%)
Abisko	24	30
Pallas	19	23
Värriö	15	21

Analysis of particle size distribution changes

R. Väänänen et al.

Table 2. Statistics of the properties of NPF events. Calculated mean, median and standard deviations, also 10% and 90% percentiles (P10–P90). Here, too, the shorter measurement periods in Abisko prevent direct comparison (see Table 1). Due to different cut-off size of the instruments, the formation rates are J_{10} , J_7 and J_3 , for Abisko, Pallas, and Värriö, respectively.

	Growth rate GR (nm h ⁻¹)			Formation rate J (cm ⁻³ s ⁻¹)		
	Mean ± Std	Median	P10–P90	Mean ± Std	Median	P10–P90
Abisko	3.7 ± 2.7	3.0	1.1–6.6	0.1 ± 0.2	0.05	0.002–0.3
Pallas	3.3 ± 2.3	2.6	1.3–6.6	0.1 ± 0.2	0.08	0.01–0.3
Värriö	2.8 ± 2.0	2.0	1.0–6.2	0.09 ± 0.08	0.07	0.02–0.2

Title Page

Abstract

Introduction

Conclusions

References

Tables

Figures

◀

▶

◀

▶

Back

Close

Full Screen / Esc

Printer-friendly Version

Interactive Discussion



Analysis of particle size distribution changes

R. Väänänen et al.

Table 3. Increase rates of mode peak diameter, accumulated mass concentration and condensation sink when airmasses travel over land. See Fig. 5.

	Abisko	Pallas	Värriö
Apparent particle growth rate (nm h^{-1}) Over-land-times used (h)	0.55 ± 0.04 12–80	0.72 ± 0.04 22–80	0.68 ± 0.05 22–80
Accumulated mass conc. increase ($\mu\text{gm}^{-3} \text{h}^{-1}$) Over-land-times used (h)	0.015 ± 0.002 5–50	0.016 ± 0.001 10–50	0.023 ± 0.001 12–50
Apparent growth of condensation sink ($\text{s}^{-1} \text{h}^{-1}$) Over-land-times used (h)	0.022 ± 0.001 5–80	0.026 ± 0.001 10–80	0.029 ± 0.001 10–80

Title Page

Abstract

Introduction

Conclusions

References

Tables

Figures

◀

▶

◀

▶

Back

Close

Full Screen / Esc

Printer-friendly Version

Interactive Discussion



Analysis of particle size distribution changes

R. Väänänen et al.

Table 4. Dynamics of particle size distributions when airmasses transport from one site to another, summer season. The initial size distributions are clustered and a log-normal fitting in the both ends of the paths is used to find the mode peak diameters and mode concentrations. In this table the changes in mode peak diameters and mode concentrations are shown.

mean Δt	mean RH		Mode peak (nm)			Concentration of mode (cm^{-3})		
			Abisko	Pallas	Shift of mode (nm h^{-1})	Abisko	Pallas	Concentration change ($\text{cm}^{-3} \text{s}^{-1}$)
Cluster 1	15 h	77 %	29	22	1.3	238	429	I+II both +0.01 −0.001
			139	48	1.3	89	415	
				158			79	
Cluster 2	13 h	77 %	60	16	0.2	270	70	−0.001 +0.004
			148	37		748	196	
				151			954	
			Pallas	Värriö		Pallas	Värriö	
Cluster 1	16 h	72 %	26	36	0.6	139	1051	+0.02
			110	163	3.3	318	92	−0.004
Cluster 2	28 h	78 %	57	57	0.0	140	543	−0.004 −0.005
			165	169	0.1	1206	667	
			Pallas	Abisko		Pallas	Abisko	
Cluster 1	22 h	85 %	22	25	−0.0	45	199	+0.002
			63	62	0.5	122	250	+0.002
			169	197		103	237	+0.002
			Värriö	Pallas		Värriö	Pallas	
Cluster 1	17 h	82 %	22	48	+1.5	78	307	I+II both +0.000 −0.000
			53	166	−0.3	210	164	
			193		−1.5	196		
Cluster 2	27 h	81 %	22	28	+0.0	57	61	II+III both −0.005
			97	98	−1.1	808	612	
			206	235		354	87	

Title Page

Abstract

Introduction

Conclusions

References

Tables

Figures

◀

▶

◀

▶

Back

Close

Full Screen / Esc

Printer-friendly Version

Interactive Discussion



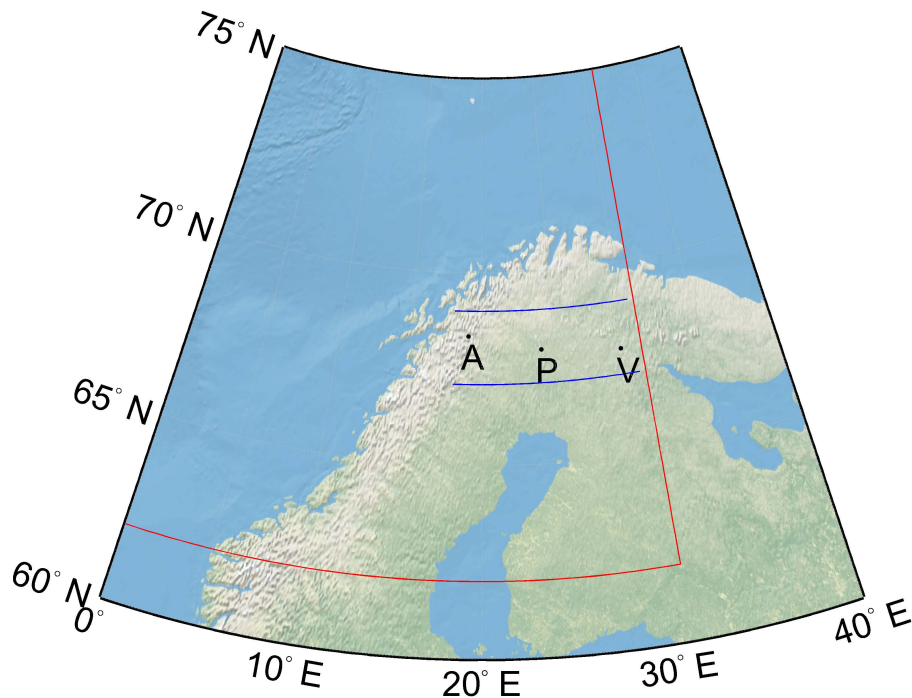


Fig. 1. A map of Northern Scandinavia. The measurement stations are located approximately in line from west to east in the following order: Abisko, Pallas, Värriö (A, P, and V in the map). Red lines show the sector from where the trajectories are accepted when studied the aerosol dynamics over the continent. Blue lines show the limits for the trajectory paths when studying aerosol dynamics between the measurement stations. (Map: Natural Earth data).

Analysis of particle size distribution changes

R. Väänänen et al.

Title Page

Abstract

Introduction

Conclusions

References

Tables

Figures

◀

▶

◀

▶

Back

Close

Full Screen / Esc

Printer-friendly Version

Interactive Discussion



Analysis of particle size distribution changes

R. Väänänen et al.

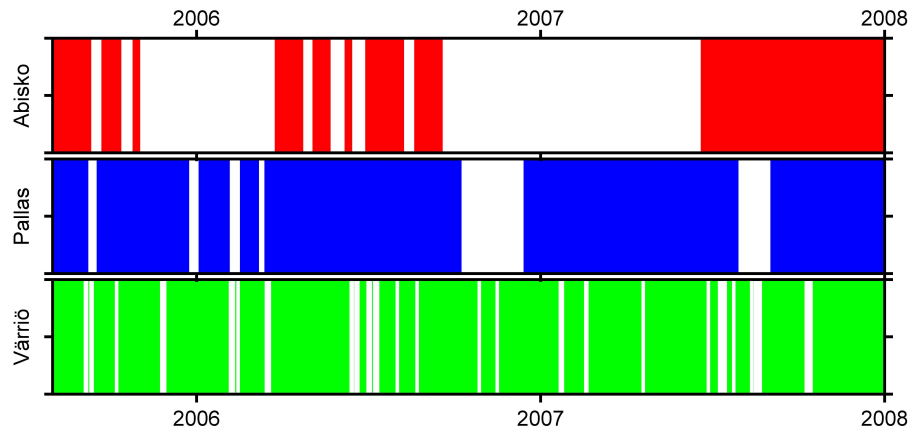


Fig. 2. Colored areas show the time intervals when particle size distribution data is available from corresponding station.

[Title Page](#)[Abstract](#)[Introduction](#)[Conclusions](#)[References](#)[Tables](#)[Figures](#)[◀](#)[▶](#)[◀](#)[▶](#)[Back](#)[Close](#)[Full Screen / Esc](#)[Printer-friendly Version](#)[Interactive Discussion](#)

Analysis of particle size distribution changes

R. Väänänen et al.

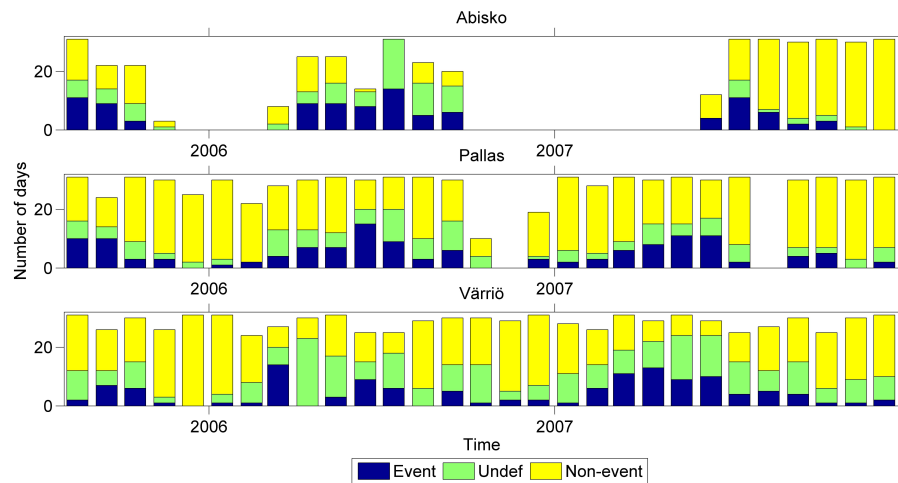


Fig. 3. Number of new particle formation (NPF) event days, non-NPF event days and undefined days in all measurement sites.

Title Page

Abstract

Introduction

Conclusions

References

Tables

Figures

◀

▶

◀

▶

Back

Close

Full Screen / Esc

Printer-friendly Version

Interactive Discussion



Analysis of particle size distribution changes

R. Väänänen et al.

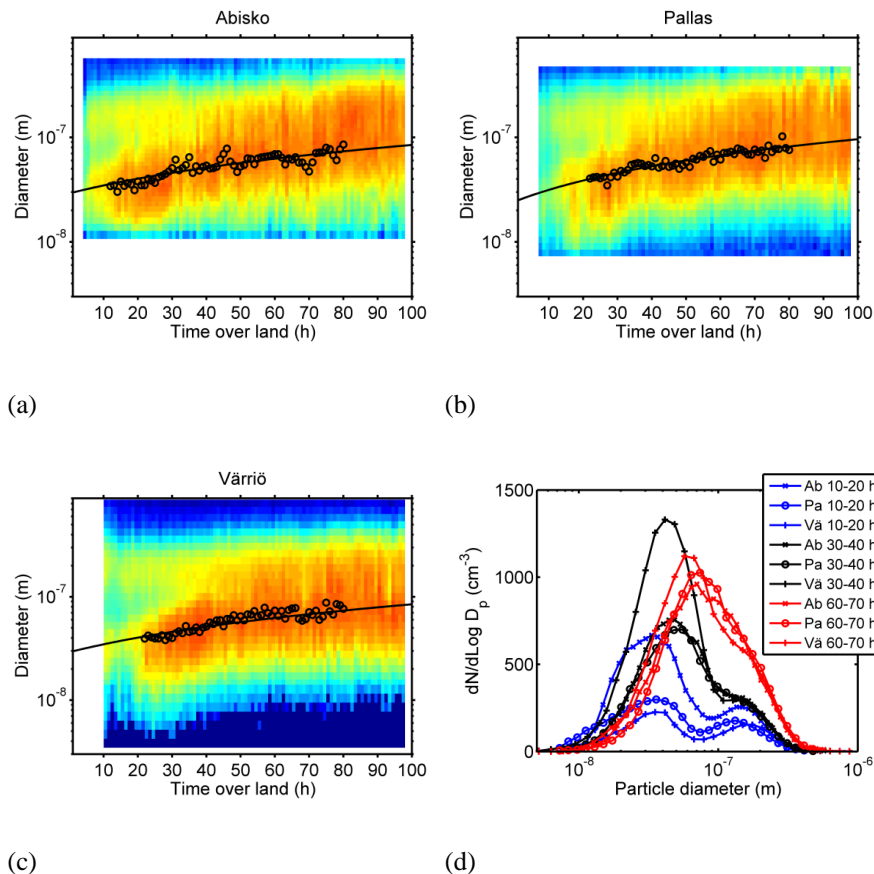
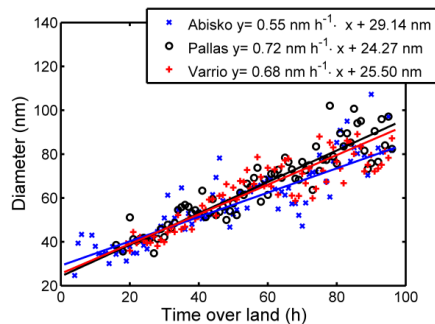


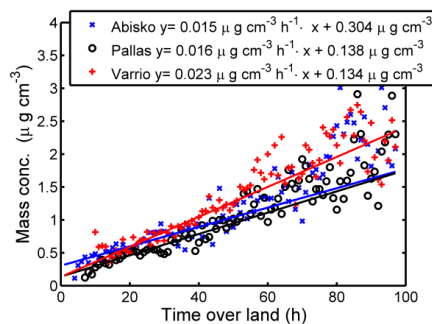
Fig. 4. (a–c) Median size distributions as a function of time the corresponding trajectory has spent over land during the last 96 h. Only summer (1 April–30 September) covered. (d) Mean size distributions for certain time periods for all station.

Analysis of particle size distribution changes

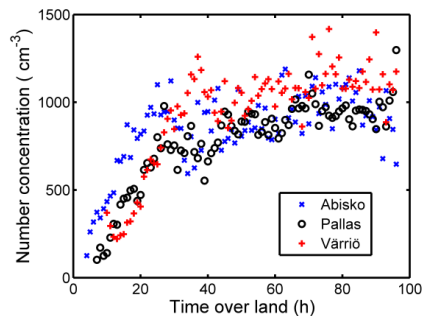
R. Väänänen et al.



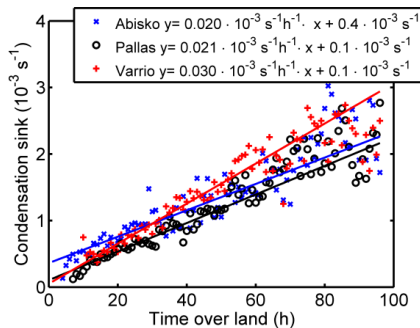
(a) Particle mode diameter



(b) Accumulated mass concentration



(c) Particle number concentration



(d) Condensation sink

Fig. 5. Particle mode diameter **(a)**, integrated mass concentrations **(b)**, number concentrations **(c)**, and condensation sink **(d)** as a function of time the corresponding air mass has spent over land.

Title Page

Abstract Introduction

Conclusions References

Tables Figures

◀ ▶

◀ ▶

Back Close

Full Screen / Esc

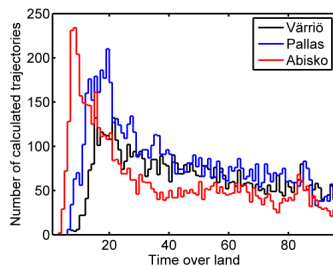
Printer-friendly Version

Interactive Discussion

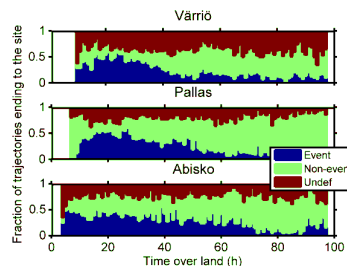


Analysis of particle
size distribution
changes

R. Väänänen et al.



a) Histogram of the on-land time of trajectories



b) Fractions of NPF event and non-event days

Fig. 6. (a) Distribution of the times the trajectories had spent over land. (b) Fractions of the trajectories that ended to each site during event, non-event, or undefined days.

[Title Page](#)[Abstract](#)[Introduction](#)[Conclusions](#)[References](#)[Tables](#)[Figures](#)[◀](#)[▶](#)[◀](#)[▶](#)[Back](#)[Close](#)[Full Screen / Esc](#)[Printer-friendly Version](#)[Interactive Discussion](#)

Analysis of particle size distribution changes

R. Väänänen et al.

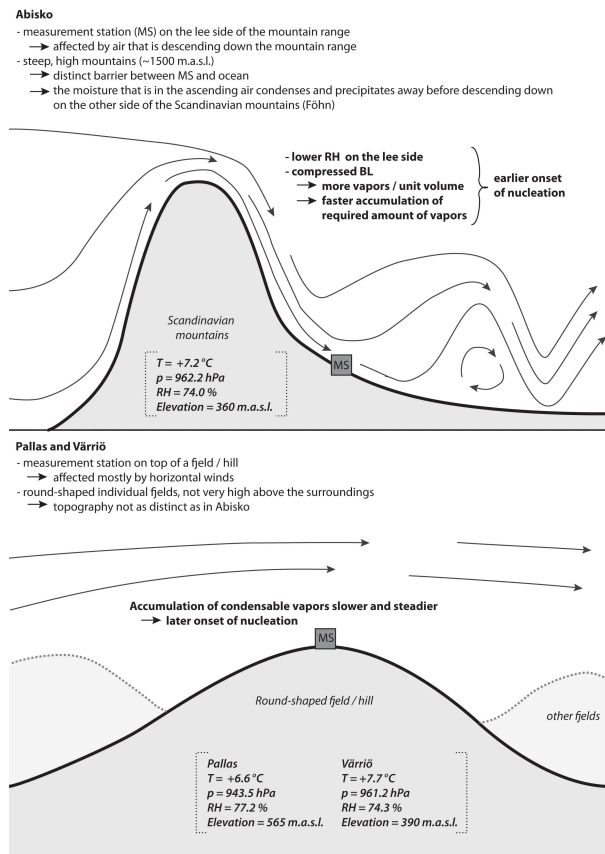


Fig. 7. General topographical and meteorological differences between Abisko as well as Pallas and Värriö stations and their effect on the onset of nucleation. Mean temperature, pressure and relative humidity are shown for the years 2005–2007 over the period 1 April–30 September for each station.

Title Page

Abstract

Introduction

Conclusions

References

Tables

Figures

◀

▶

◀

▶

Back

Close

Full Screen / Esc

Printer-friendly Version

Interactive Discussion

Analysis of particle size distribution changes

R. Väänänen et al.

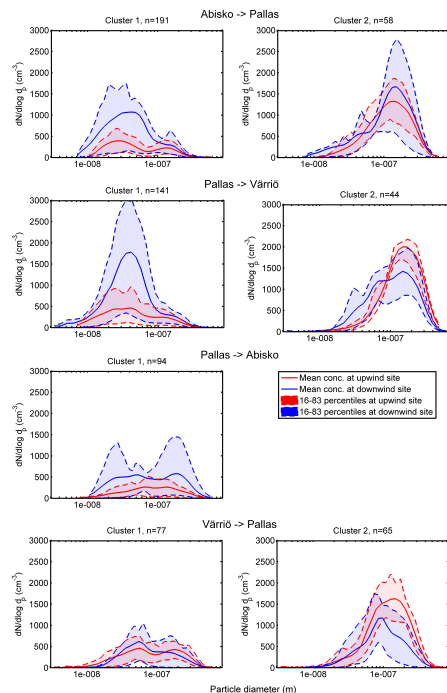


Fig. 8. The dynamics of particle size distributions when air masses are moving from one measurement site to another. Summer season 1 April–30 September covered. The initial size distributions at the upwind station are clustered to obtain as similar initial states as possible. Each subplot represents one cluster. The first one of the site pair is the upwind site, and the second one is the downwind site. The cluster mean size distribution at the upwind station is plotted with solid red line, and the shadowed red area shows the percentiles between 16 and 83. Similarly, blue solid line is the mean of the corresponding size distributions at the downwind station, and shadowed blue area shows the above mentioned percentiles. The number n shows the amount of size distribution pairs in each cluster.

Title Page

Abstract

Introduction

Conclusions

References

Tables

Figures

◀

▶

◀

▶

Back

Close

Full Screen / Esc

Printer-friendly Version

Interactive Discussion

Analysis of particle size distribution changes

R. Väänänen et al.

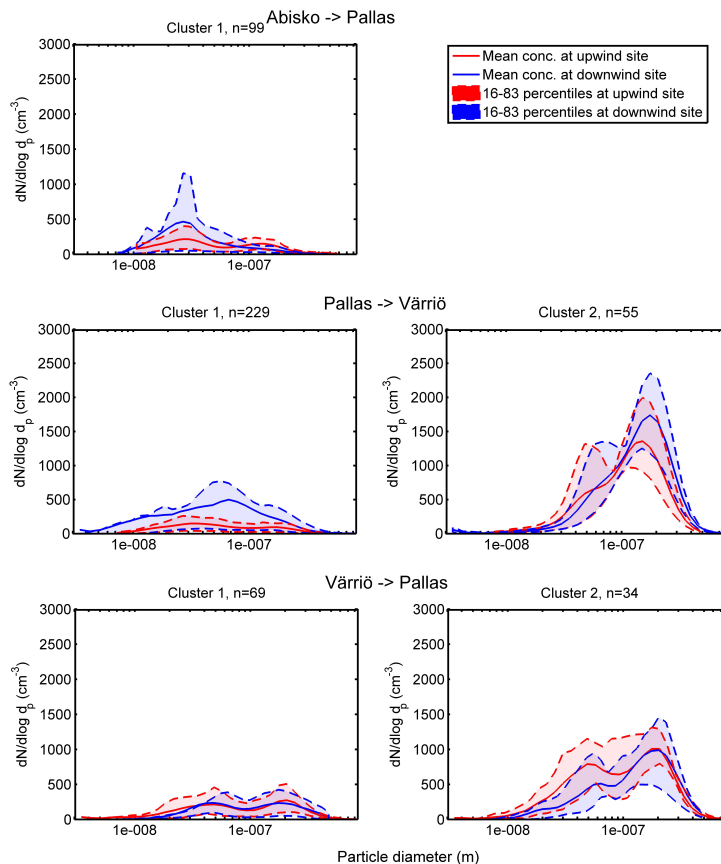


Fig. 9. The dynamics of particle size distributions when airmasses are moving from one measurement site to another. Similar to Fig. 8, but winter season 1 October–31 March covered.

Title Page

Abstract Introduction

Conclusions References

Tables Figures

◀ ▶

◀ ▶

Back Close

Full Screen / Esc

Printer-friendly Version

Interactive Discussion

